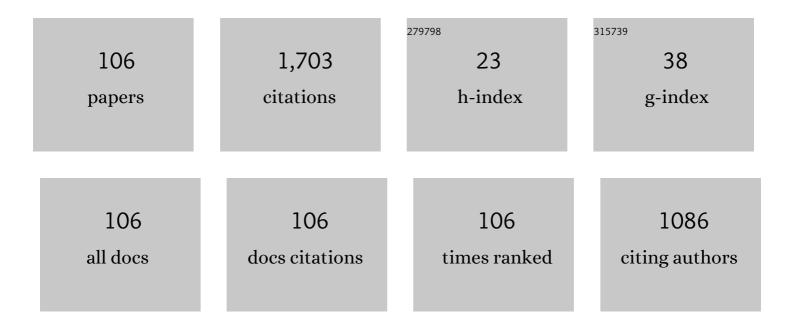
List of Publications by Year in descending order

Source: https://exaly.com/author-pdf/8913155/publications.pdf Version: 2024-02-01



#	Article	IF	CITATIONS
1	A security evaluation model for multi-source heterogeneous systems based on IOT and edge computing. Cluster Computing, 2023, 26, 303-317.	5.0	6
2	Artificial neural networks assisting the design of a dual-mode photonic crystal nanobeam cavity for simultaneous sensing of the refractive index and temperature. Applied Optics, 2022, 61, 4802.	1.8	9
3	Portable Automatic Microring Resonator System Using a Subwavelength Grating Metamaterial Waveguide for High-Sensitivity Real-Time Optical-Biosensing Applications. IEEE Transactions on Biomedical Engineering, 2021, 68, 1894-1902.	4.2	13
4	High sensitivity and anti-external interference dual-parameter sensor based on a multimode slotted photonic crystal nanobeam cavity. Journal of Modern Optics, 2021, 68, 357-364.	1.3	4
5	Simultaneous detection of complex refractive index and temperature using a compact side-coupled photonic crystal nanobeam cavity. Journal of the Optical Society of America B: Optical Physics, 2021, 38, 2765.	2.1	3
6	Artificial neural networks applied in fast-designing ultrabroad bandgap elliptical hole dielectric mode photonic crystal nanobeam cavity. Applied Optics, 2021, 60, 8977.	1.8	2
7	High Figure of Merit Magnetic Field Sensor Based on Photonic Crystal Slab Supporting Quasi Bound States in The Continuum. , 2021, , .		0
8	Analysis About Low Differential Mode Delay Based on Wavelength Dependence of Effective Refractive Index in Few Mode Fibers Around 1550nm. , 2021, , .		0
9	Highly Sensitive 1 × 8 Parallel Multiplexing of Ultra-Compact Integrated 1D Photonic Crystal Sensor Array Based on Silicon-on-Insulator Platform. IEEE Access, 2020, 8, 65179-65186.	4.2	3
10	Anti-external interference sensor based on cascaded side-coupled photonic crystal nanobeam cavities for simultaneous sensing of the refractive index and temperature. Journal of the Optical Society of America B: Optical Physics, 2020, 37, 3850.	2.1	4
11	Modeling and design of a coupled PhC slab sensor for simultaneous detection of refractive index and temperature with strong anti-interference ability. Optics Express, 2020, 28, 22151.	3.4	8
12	Inverse design of a bend-resistant low bending loss and large mode area single-mode fiber by Neural Network. , 2020, , .		0
13	Ultra-compact Sensor Based on a single-cavity dual-mode Photonic Crystal Nanobeam for Simultaneous Detection of Relative Humidity and Temperature. , 2020, , .		Ο
14	Side-coupled nanoscale photonic crystal structure with high-Q and high-stability for simultaneous refractive index and temperature sensing. Journal of Modern Optics, 2019, 66, 1339-1346.	1.3	13
15	Load-balanced adaptive routing flexible grouping spectrum and core assignment in SDM-EONs based on mixed super-channel. Optical Fiber Technology, 2019, 51, 6-16.	2.7	5
16	Anti-External Interference Sensor Based on Cascaded Photonic Crystal Nanobeam Cavities for Simultaneous Detection of Refractive Index and Temperature. Journal of Lightwave Technology, 2019, 37, 2209-2216.	4.6	21
17	Bandwidth-Enhanced PAM-4 Transmissions Using Polarization Modulation and Direct Detection With a Tunable Frequency Range. Journal of Lightwave Technology, 2019, 37, 1014-1022.	4.6	8
18	High-sensitivity broad free-spectral-range two-dimensional three-slot photonic crystal sensor integrated with a 1D photonic crystal bandgap filter. Applied Optics, 2019, 58, 5997.	1.8	8

#	Article	IF	CITATIONS
19	Double-layer Fano resonance photonic-crystal-slab-based sensor for label-free detection of different size analytes. Journal of the Optical Society of America B: Optical Physics, 2019, 36, 215.	2.1	10
20	Simultaneous sensing of refractive index and temperature based on a three-cavity-coupling photonic crystal sensor. Optics Express, 2019, 27, 26471.	3.4	21
21	Wide stopband miniaturized "lâ€â€ŧyped EBG with DGS. Microwave and Optical Technology Letters, 2018, 60, 44-50.	1.4	5
22	An Effective Artificial Neural Network Equalizer with S-shape Activation Function for High-speed 16-QAM Transmissions using Low-cost Directly Modulated Laser. , 2018, , .		2
23	An Artificial Neural Network MIMO Demultiplexer for Small-Cell MM-Wave RoF Coordinated Multi-Point Transmission System. , 2018, , .		2
24	Large-Dynamic-Range Dual-Parameter Sensor Using Broad FSR Multimode Photonic Crystal Nanobeam Cavity. IEEE Photonics Journal, 2018, 10, 1-14.	2.0	8
25	A Long-Distance Millimeter-Wave RoF System With a Low-Cost Directly Modulated Laser. IEEE Photonics Technology Letters, 2018, 30, 1396-1399.	2.5	17
26	A bend-resistant low bending loss and large mode area two-layer core single-mode fiber with gradient refractive index ring and multi-trench. Optical Fiber Technology, 2018, 45, 235-243.	2.7	7
27	Multiplexing dual-parameter sensor using photonic crystal multimode nanobeam cavities. Optics Communications, 2018, 427, 382-389.	2.1	11
28	A Novel ANN Equalizer to Mitigate Nonlinear Interference in Analog-RoF Mobile Fronthaul. IEEE Photonics Technology Letters, 2018, 30, 1675-1678.	2.5	27
29	Simultaneous detection of refractive index, temperature and stress realized by using a three-mode planar photonic crystal L5 cavity. Optics Communications, 2018, 427, 13-20.	2.1	8
30	Mitigation of Multi-user Access Impairments in 5G A-RoF-based Mobile Fronthaul utilizing Machine Learning for an Artificial Neural Network Nonlinear Equalizer. , 2018, , .		17
31	Realization of Tunable Frequency Response in Polarization Modulation and Direct Detection Scheme for High-speed Optical Access System. , 2018, , .		4
32	A Wide Band-Gap Slot Fractal UC-EBG Based on Moore Space-Filling Geometry for Microwave Application. IEEE Antennas and Wireless Propagation Letters, 2017, 16, 33-37.	4.0	18
33	Parabolic Tapered Coupled Two Photonic Crystal Nanobeam Slot Cavities for High-FOM Biosensing. IEEE Photonics Technology Letters, 2017, 29, 1281-1284.	2.5	23
34	Design on-chip width-modulated line-defect cavity array structure for multiplexing complex refractive index sensing. Sensors and Actuators A: Physical, 2017, 257, 8-14.	4.1	13
35	Low detection limit sensor based on subwavelength grating racetrack resonator. , 2017, , .		2
36	Design of side-coupled cascaded photonic crystal sensors array with ultra-high figure of merit. Optics Communications, 2017, 392, 68-72.	2.1	10

HUIPING TIAN

#	Article	IF	CITATIONS
37	A potential candidate design for nanosecond-order delay based on high-group index four rows optimized air holes line-defect photonic crystal waveguide. Journal of Modern Optics, 2017, 64, 1419-1428.	1.3	0
38	Silicon based On-chip Sub-Wavelength Grating Ring and Racetrack Resonator BioSensors. MRS Advances, 2017, 2, 1577-1589.	0.9	4
39	A Multilevel Artificial Neural Network Nonlinear Equalizer for Millimeter-Wave Mobile Fronthaul Systems. Journal of Lightwave Technology, 2017, 35, 4406-4417.	4.6	53
40	High figure of merit ultra-compact 3-channel parallel-connected photonic crystal mini-hexagonal-H1 defect microcavity sensor array. Optics Communications, 2017, 396, 71-77.	2.1	13
41	Capacity allocation mechanism based on differentiated QoS in 60 GHz radio-over-fiber local access network. Optics Communications, 2017, 387, 290-295.	2.1	2
42	Highly sensitive one chip eight channel sensing of ultra-compact parallel integrated photonic crystal cavities based on silicon-on-insulator platform. , 2017, , .		0
43	Ultra-compact dual-parameter sensing based on a photonic crystal rectangular holes nanobeam multimode microcavity. , 2017, , .		1
44	An Adaptive Activated ANN Equalizer Applied in Millimeter-Wave RoF Transmission System. IEEE Photonics Technology Letters, 2017, 29, 1935-1938.	2.5	20
45	Improving the detection limit for on-chip photonic sensors based on subwavelength grating racetrack resonators. Optics Express, 2017, 25, 10527.	3.4	84
46	Ultra-compact air-mode photonic crystal nanobeam cavity integrated with bandstop filter for refractive index sensing. Applied Optics, 2017, 56, 4363.	2.1	21
47	A load-balanced adaptive routing and wavelength assignment algorithm based on cost updating. , 2017, , .		0
48	Subwavelength grating racetrack resonator based ultrasensitive refractive index sensor. , 2017, , .		0
49	Multiplexed Simultaneous High Sensitivity Sensors with High-Order Mode Based on the Integration of Photonic Crystal 1 × 3 Beam Splitter and Three Different Single-Slot PCNCs. Sensors, 2016, 16, 1050.	3.8	25
50	Unique surface sensing property and enhanced sensitivity in microring resonator biosensors based on subwavelength grating waveguides. Optics Express, 2016, 24, 29724.	3.4	101
51	A 60-GHz RoF System With Blind VSS-DD-LMS Equalizer for Optical-Wireless Transmission. IEEE Photonics Technology Letters, 2016, 28, 2383-2386.	2.5	3
52	Performance investigation of side-coupled interlaced symmetric-shaft-shape photonic crystal sensor arrays. Optics Communications, 2016, 381, 146-151.	2.1	11
53	Special cascade LMS equalization scheme suitable for 60-GHz RoF transmission system. Optics Express, 2016, 24, 10599.	3.4	12
54	Optimization of One Dimensional Photonic Crystal Elliptical-Hole Low-Index Mode Nanobeam Cavities for On-Chip Sensing. Journal of Lightwave Technology, 2016, 34, 3496-3502.	4.6	40

#	Article	IF	CITATIONS
55	A 60-GHz RoF System Employing Variable Step Size LMS Equalizer with Fast Convergence Speed. , 2016, , .		3
56	High-Q, high sensitivity and wide bandgap low-index-mode elliptical holes photonic crystal nanobeam cavities biosensors. , 2016, , .		0
57	Higher Q factor and higher extinction ratio with lower detection limit photonic crystal–parallel-integrated sensor array for on-chip optical multiplexing sensing. Applied Optics, 2016, 55, 10078.	2.1	2
58	Ultrahigh- <inline-formula> <tex-math notation="LaTeX"&gt;\$Q\$</tex-math </inline-formula> and Low-Mode-Volume Parabolic Radius-Modulated Single Photonic Crystal Slot Nanobeam Cavity for High-Sensitivity Refractive Index Sensing. IEEE Photonics Journal, 2015, 7, 1-8.	2.0	28
59	Radius vertical graded nanoscale interlaced-coupled photonic crystal sensors array. Optics Communications, 2015, 355, 331-336.	2.1	16
60	Multi-directional ultra-high sensitive pressure sensor based on the integration of optimized double 60° bend waveguides and modified center-defect photonic crystal microcavity. Photonics and Nanostructures - Fundamentals and Applications, 2015, 15, 116-123.	2.0	1
61	Photonic crystal nanoslotted parallel quadrabeam integrated cavity for refractive index sensing with high figure of merit. Photonics and Nanostructures - Fundamentals and Applications, 2015, 15, 124-129.	2.0	3
62	High-Q and high-sensitivity width-modulated photonic crystal single nanobeam air-mode cavity for refractive index sensing. Applied Optics, 2015, 54, 1.	1.8	86
63	Bandwidth and gain enhancement of optically transparent 60-GHz CPW-fed antenna by using BSIS-UC-EBG structure. Photonics and Nanostructures - Fundamentals and Applications, 2015, 15, 99-108.	2.0	1
64	Label-free optical sensor by designing a high-Q photonic crystal ring–slot structure. Optics Communications, 2015, 335, 73-77.	2.1	87
65	A 60-GHz RoF System Providing 5-Gbps BPSK Signal Employing LMS Equalizer. , 2015, , .		1
66	Design Low Crosstalk Ring-Slot Array Structure for Label-Free Multiplexed Sensing. Sensors, 2014, 14, 15658-15668.	3.8	27
67	Refractive index sensing utilizing parallel tapered nano-slotted photonic crystal nano-beam cavities. Journal of the Optical Society of America B: Optical Physics, 2014, 31, 1746.	2.1	31
68	Low-loss, efficient, wide-angle 1  ×  4 power splitter at â^¼155  μm wavelength with a monolithic photonic crystal slab. Applied Optics, 2014, 53, 8012.	s for four p	lay application
69	Wide-bandwidth, high-gain, low-temperature cofired ceramic magneto-electric dipole antenna and arrays for millimeter wave radio-over-fiber systems. Photonics Research, 2014, 2, B40.	7.0	4
70	Nanoscale Low Crosstalk Photonic Crystal Integrated Sensor Array. IEEE Photonics Journal, 2014, 6, 1-7.	2.0	26
71	Integration of high transmittance photonic crystal H2 nanocavity and broadband W1 waveguide for biosensing applications based on Silicon-on-Insulator substrate. Optics Communications, 2014, 330, 175-183.	2.1	31
72	High sensitivity and high <i>Q</i> -factor nanoslotted parallel quadrabeam photonic crystal cavity for real-time and label-free sensing. Applied Physics Letters, 2014, 105, .	3.3	92

#	Article	IF	CITATIONS
73	Optimization of figure of merit in label-free biochemical sensors by designing a ring defect coupled resonator. Optics Communications, 2014, 332, 42-49.	2.1	43
74	Ultra-broadband and ultra-low-loss photonic crystal with band-flatness waveguide 60° bend obtained based on lattice-shifted optimization. Optics Communications, 2014, 322, 227-233.	2.1	10
75	Ultra-compact low-voltage and slow-light MZI electro-optic modulator based on monolithically integrated photonic crystal. Optics Communications, 2014, 315, 138-146.	2.1	1
76	Nanomechanical three dimensional force photonic crystal sensor using shoulder-coupled resonant cavity with an inserted pillar. Sensors and Actuators A: Physical, 2014, 209, 33-40.	4.1	20
77	Nanoscale radius-graded photonic crystal sensor arrays using interlaced and symmetrical resonant cavities for biosensing. Sensors and Actuators A: Physical, 2014, 216, 223-230.	4.1	18
78	Ultracompact ring resonator microwave photonic filters based on photonic crystal waveguides. Applied Optics, 2013, 52, 1218.	1.8	9
79	Wideband quasi-isotropic H-shaped slot fractal UC-EBGs with alternately arranged symmetrical unit cells. Journal of Electromagnetic Waves and Applications, 2013, 27, 962-968.	1.6	3
80	Bandwidth Enhancement of Monopole UWB Antenna With New Slots and EBG Structures. IEEE Antennas and Wireless Propagation Letters, 2013, 12, 1550-1553.	4.0	49
81	EBG ME-dipole antenna with enhanced gain for intelligent radio-over-fiber systems. , 2013, , .		1
82	Photonic crystal stress sensor with high sensitivity in double directions based on shoulder-coupled aslant nanocavity. Sensors and Actuators A: Physical, 2013, 193, 149-154.	4.1	35
83	Nanoscale torsion-free photonic crystal pressure sensor with ultra-high sensitivity based on side-coupled piston-type microcavity. Sensors and Actuators A: Physical, 2013, 199, 30-36.	4.1	36
84	A tnnable electro-optic microwave photonic filter based on photonic crystal for 60GHz radio over fiber system. , 2013, , .		1
85	Design of simultaneous high-Q and high-sensitivity photonic crystal refractive index sensors. Journal of the Optical Society of America B: Optical Physics, 2013, 30, 2027.	2.1	49
86	Broadband and low-power bright soliton propagation in line-defect photonic crystal waveguide. Optical Engineering, 2013, 52, 055006.	1.0	1
87	Integration of Photonic Crystal Splitter and Slow Light Waveguide for a Microwave Photonic Filter. IEEE Photonics Journal, 2013, 5, 5501311-5501311.	2.0	2
88	Infrared perfect metamaterial absorber and its potential application as strain sensor. , 2013, , .		0
89	Ultra-high-transmittance and High-extinction-ratio Biosensor Based on Photonic Crystal Slab Using H2-type Resonator. , 2013, , .		0
90	Soliton propagation optimization and dynamic modulation in photonic crystal waveguide with polystyrene background. Optics Communications, 2012, 285, 171-177.	2.1	4

#	Article	lF	CITATIONS
91	Tunable slow light and buffer capability in photonic crystal coupled-cavity waveguides based on electro-optic effect. Optics Communications, 2012, 285, 2760-2764.	2.1	17
92	High-bandwidth and low-loss photonic crystal power-splitter with parallel output based on the integration of Y-junction and waveguide bends. Optics Communications, 2012, 285, 3752-3757.	2.1	35
93	Research on the Dispersion Compensation of Slot Photonic Crystal Waveguide. IEEE Photonics Technology Letters, 2011, 23, 1222-1224.	2.5	9
94	Slow Light Property Improvement and Optical Buffer Capability in Ring-Shape-Hole Photonic Crystal Waveguide. Journal of Lightwave Technology, 2011, 29, 3083-3090.	4.6	64
95	Nanoscale photonic crystal sensor arrays on monolithic substrates using side-coupled resonant cavity arrays. Optics Express, 2011, 19, 20023.	3.4	91
96	The study of electro-optical sensor based on slotted photonic crystal waveguide. Optics Communications, 2011, 284, 4986-4990.	2.1	10
97	The properties of lattice-shifted microcavity in photonic crystal slab and its applications for electro-optical sensor. Sensors and Actuators A: Physical, 2011, 171, 146-151.	4.1	22
98	Group index and dispersion properties of photonic crystal waveguides with circular and square air-holes. Optics Communications, 2010, 283, 1768-1772.	2.1	12
99	The properties and structure optimization of slot photonic crystal waveguide. , 2010, , .		0
100	Dynamic tuning of slow light transmission in manual nanostructure photonic crystal waveguide. International Journal of Nanotechnology, 2009, 6, 715.	0.2	0
101	Investigation of slow light utilized as optical storage in photonic crystal coupled resonator optical waveguide. , 2008, , .		0
102	Dynamic tuning of slow light transmission in manual nanostructure photonic crystal waveguide. , 2008, , .		0
103	Ultra-narrow bandwidth filter in fractal photonic crystal containing negative material. , 2008, , .		0
104	The effects on band gaps for the cross section's Shape of the medium column in 2-D photonic crystals. , 2008, , .		0
105	Wide-band transmission of slow light in one-dimensional photonic crystal coupled resonator optical waveguide. , 2007, , .		0
106	Improved line defect structures for slow light transmission in photonic crystal waveguide. Optics Communications, 2007, 279, 214-218.	2.1	14